# A photon-counting time-of-flight ranging technique developed for the avoidance of range ambiguity at gigahertz clock rates

**Philip A. Hiskett[1,2*], Colin S. Parry[1], Aongus McCarthy[1] and Gerald S. Buller[1**]**

*[1]School of Engineering and Physical Sciences, Heriot-Watt University, Riccarton, Edinburgh, UK, EH14 4AS*
*[2]Currently with SELEX Galileo, Crewe Toll, Ferry Road, Edinburgh, UK, EH5 2XS*
**Corresponding author: philip.hiskett@selex-sas.com*
*** Corresponding author: G.S.Buller@hw.ac.uk*

**Abstract:** This paper describes a rapid data acquisition photon-counting time-of-flight ranging technique that is designed for the avoidance of range ambiguity, an issue commonly found in high repetition frequency time-of-flight systems. The technique transmits a non-periodic pulse train based on the random bin filling of a high frequency time clock. A received pattern is formed from the arrival times of the returning single photons and the correlation between the transmitted and received patterns was used to identify the unique target time-of-flight. The paper describes experiments in laboratory and in free space at over several hundred meters range at clock frequencies of 1GHz. Unambiguous photon-counting range-finding is demonstrated with centimeter accuracy.



**OCIS codes:** (120.0280) Remote sensing and sensors; (280.3400) Laser range finder; (280.3640) Lidar; (030.5260) Photon counting; (040.3780) Low light level; (070.5010) Pattern recognition; (120.3940 Metrology); (100.4999) Pattern recognition, target tracking

## References and links

1. J. S. Massa, A. M. Wallace, G. S. Buller, S. J. Fancey and A. C. Walker, "Laser depth measurement based on time-correlated single photon counting," Opt. Lett. **22**, 543 (1997)
2. G. S. Buller, R. D. Harkins, A. McCarthy, P. A. Hiskett, G. R. MacKinnon, G. R. Smith, R. Sung, A. M. Wallace, R. A. Lamb, K. A. Ridley and J. G. Rarity, "A multiple wavelength time-of-flight sensor based on time-correlated single-photon counting," Rev. Sci. Instrum. **76**, 083112-083112-7 (2005).
3. G. S. Buller and A. M. Wallace "Recent advances in Ranging and Three-Dimensional imaging using time-correlated single-photon counting," J. Sel. Top. Quantum Electron., **13**, 1006-1015, (2007)
4. R. E. Warburton, A McCarthy, A. M. Wallace, S. Hernandez-Marin, R. H. Hadfield, S. W. Nam, and G. S. Buller, "Sub-centimeter depth resolution using a single-photon counting time-of-flight laser ranging system at 1550nm wavelength," Opt. Lett, **32**, 2266-2268 (2007).
5. "GT6558, PC-based Time Interval Analyzer," http://www.jitter.com/products/pcBase/658_1.htm
6. C. Elachi, J. Van Zyl, *Introduction to the Physics and Techniques of Remote Sensing*, 2nd Edition, (John Wiley & Sons, 2006), 232-234.
7. C. H. Bennett and G. Brassard, "Quantum Cryptography: Public-key distribution and coin tossing," Proc. IEEE Int. Conf. on Computers, Systems and Signal Proc 175 – 179, (1984).
8. R. J. Hughes, T. E. Chapuran, N. Dallmann, P. A. Hiskett, K. P. McCabe, P. M. Montano, J. E. Nordholt, C.G. Peterson, R. J. Runser, R.Sedillo, K. Tyagi, C. C. Wipf, "A quantum key distribution system for optical fiber networks," Proc. SPIE Quantum Communication and Quantum Imaging **5893,** 589301.1-589301.10 (2005).
9. P. A. Hiskett, C. G. Peterson, D. Rosenberg, S. Nam, A. E. Lita, A. J. Miller, R. J. Hughes, J. E. Nordholt, "A novel switched interferometric quantum key distribution system," Proc SPIE Quantum Communication and Quantum Imaging V. **6710**, 67100S-67100S-12 (2007).
10. G. W. Stimson, *Introduction to Airborne Radar*, 2nd Ed. (SciTech Publishing Inc, 1998), pp. 156-157.
11. S. Pellegrini, G. S. Buller, J. M. Smith, A. M. Wallace, and S. Cova, "Laser-based distance measurement using picosecond resolution time-correlated single-photon counting," Meas. Sci. Technol. **11**, 712-716 (2000).
12. M. Ghioni, A. Gulinatti, I. Rech, F. Zappa, and S. Cova, "Progress in silicon single-photon avalanche diodes,", IEEE J. Sel. Top. Quantum Electron. **13**, 852-862 (2007).

#94106 - $15.00 USD Received 20 Mar 2008; revised 27 Jun 2008; accepted 23 Jul 2008; published 21 Aug 2008

## 1. Introduction to time-of-flight ranging using single photon counting

Optical time-of-flight ranging using time-correlated single photon counting (TCSPC) has been shown to exhibit highly accurate range-finding with non-cooperative targets in both the laboratory at short-range [1] and within outdoor kilometer range situations [2]. This approach is consistent with the expected low target return from non-cooperative targets and utilizes the high statistical accuracy inherent in the TCSPC technique to achieve good temporal and range resolution. Furthermore, with the appropriate signal processing algorithms the technique has the potential for identification of distributed targets without *a priori* knowledge of the target profile [3].

Whilst this approach has demonstrated excellent surface-to-surface resolution at long range, a major weakness in the TCSPC approach is the potential for ambiguity in range measurement caused by the uncertainty in synchronizing with an incorrectly assigned laser pulse in these periodically pulsed systems. In order to completely avoid the possibility of ambiguity, we must restrict the laser repetition frequency such that only one pulse is in transit at one time. Of course, at a one kilometer range the round-trip transit time is 6.66μs, restricting the laser pulse frequency to less than 150kHz. Such a low repetition rate can greatly reduce the rapidity of range data collection and the effectiveness of the overall photon-counting time-of-flight technique. In previous work [1-4], such systems have utilized periodically pulsed laser sources, typically at 10's MHz, and returned photons are timed with respect to a known reference signal. In these systems, a time-to-amplitude (TAC) based TCSPC system was used. Here, the TAC was configured in several ways, for example in some configurations the timing process was initiated by a signal from the laser driver with a fixed delay and stopped by the photon event. Alternatively, the timing process was started by the photon event and stopped by the next clock pulse from the laser driver. In either case, to fully avoid range ambiguity the user relied on *a priori* knowledge of the approximate range, either to set the fixed delays or the laser repetition frequency. In the case of targets with multiple ranges – for example targets with significant depth or rapidly moving targets – such an approach becomes extremely problematic.

In this paper we describe an alternative technique which uses a finite non-periodic pulse train and compare the received pattern to the transmitted pattern. By using a non-periodic pattern of length greater than the pulse transit time, it was possible to determine the time-of-flight and hence range in an unambiguous manner. Of course this relies on a target with a suitable cross section and a reasonable level of background counts. In this approach we utilized a time-stamping board (TSB) where a single reference pulse is used to synchronize the board and each detector event is time-stamped with respect to this pulse. To accurately maintain synchronization, the laser driver and the TSB are phased-locked by an external clock, usually a 10MHz clock. The technique was used to determine the length of a reel of ~2.2 kilometers fiber optic cable and to determine the time-of-flight of returns from a test object positioned at a distance of ~330 meters from the sensor in an outdoor environment.

## 2. Experimental method

A random pattern of length 96000 was generated in software and uploaded into a pulse pattern generator (Agilent 81134a). The probability of a binary '1' output in the pattern, known as the random number threshold, was variable but maintained at 0.1 for the experiments outlined in this paper. The output pattern from the pulse pattern generator (PPG) was in the form of a 1GHz return-to-zero bit stream, with each 1 bit corresponding to an output pulse of ~190ps duration which was then combined with a low direct current to gain-switch the vertical cavity surface emitting laser (VCSEL). The emitted optical pulses were at a wavelength of 849nm and pulse duration was ~100ps full width at half maximum (FWHM). A reference pulse correlated to the start of the output pattern was generated by the PPG and used to arm the TSB (GuideTech GT658). The PPG and TSB were phase-locked using a shared external clock. The single photons were detected using a Perkin-Elmer silicon single photon avalanche diode

#94106 - $15.00 USD Received 20 Mar 2008; revised 27 Jun 2008; accepted 23 Jul 2008; published 21 Aug 2008

(SPAD) detector, whose output was time-stamped by the TSB with respect to the arm pulse. To test the system in a controlled laboratory environment, the technique was evaluated using a reel of optical fiber of approximately 2.2km in length as the optical transmission medium. An attenuator was used to attenuate the pulse so that, on average, less than a single photon per laser pulse reached the SPAD and the output from a continuous wave (CW) source was coupled into the transmission fiber to introduce a controlled level of background counts at the SPAD. The fiber test system is shown in Fig. 1.

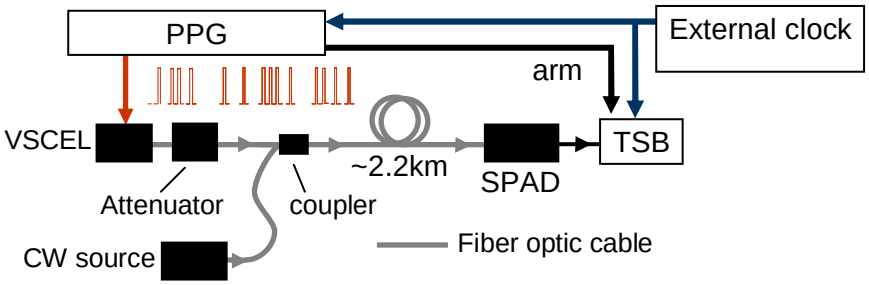


Fig. 1. A schematic of the system used to determine length of a reel of optical fiber. The pulse pattern generator (PPG) and time-stamping board (TSB) were phase locked using an external clock. A random pattern of 96000 bits was generated with a clock frequency of 1GHz and uploaded into the PPG. The probability of a '1' bit in the pattern was determined by the random number threshold which was set to 0.1. An attenuator was used to attenuate the pulse so that, on average, less than a single photon per laser pulse reaches the single photon avalanche diode (SPAD). A continuous wave (CW) source was used to introduce background counts at the SPAD. The laser pulses were coupled into a ~2.2km reel of single mode optical fiber and coupled into the SPAD. The clicks from the SPAD were time-stamped by a Guidetech GT658 TSB.

The SPAD was capable of count rates >1x10$^6$ counts per second (c/s) and the TSB has a maximum count rate of 3.5x10$^6$ c/s per channel (dead time ~286ns) [5]. In these experiments only one channel was used, however, the output from one SPAD can be split into the two channels of the TSB. Alternatively, the output from the fiber can be split using a fiber coupler and two SPADs, each connected to a single TSB channel thus theoretically increasing the maximum count rate of the system up to a maximum of 7x10$^6$ c/s. The dark count of the SPAD detector was measured to be 220 c/s.

The time-stamps of the detected photons were used to form a received pattern. To form this received pattern a random subset of the time-stamps were selected and assigned an index value equivalent to the nearest 1ns-clock reference, i.e. the nearest integer number of clock cycles elapsed since the arm pulse. Note that the laser output pulse pattern is synchronous to the 1ns-clock reference pulses. The indices in the received pattern were greater than the original indices in the transmitted pattern by the time-of-flight, at least to an integer number of clock periods. To determine the time-of-flight, the indices of the received pattern were successively decreased by 1 and the correlation between the received and transmitted pattern determined at each offset position. This process was repeated until the time-of-flight was successfully identified by an increased level of correlations at a particular offset of the received pattern.

An analogous technique is used in radar [6] where the periodic output signal is modulated by a pre-determined binary pattern which applies a 180° phase shift to the output signal for each 1-value in the binary pattern. At the receiver, the returns are passed through a tapped delay line where some of the taps have a phase shift of 180° applied. These phase shifts are distributed in the same pattern as the phase shifts were applied for the transmission signal. The received pattern is compared to the transmitted pattern as it is passed through the delay line. A high output occurs when the two patterns align.

#94106 - $15.00 USD Received 20 Mar 2008; revised 27 Jun 2008; accepted 23 Jul 2008; published 21 Aug 2008

Another analogous technique can be found in quantum key distribution (QKD) where in order to successfully sift [7], the transmitter and receiver must ensure correct synchronization to discuss the basis sets of individual bits in order to establish a shared cryptographic key. The arrival time of each received bit – an encoded photon - is offset from the corresponding transmission clock cycle by the time-of-flight of the photons in the fiber and other fixed delays associated with the receiver. A similar pattern recognition technique has been used in experimental demonstrations of QKD where the transmitter and receiver can exchange a test key and the correlation between the transmitted and received key, revealed in the minimization of the quantum bit error rate, be investigated to reveal the offset between the keys [8, 9].

In the ranging system reported in this paper, the random assignment of binary "1" outputs in the transmitted pattern was a method of 'tagging' [10] the individual outputs of the VCSEL. A comparison between a single received event, caused by the detection of a signal photon, and a single transmitted laser pulse cannot yield unambiguous information about the time-of-flight. Instead, the relative temporal position of received events compared to the relative position of transmitted laser pulses allows the time-of-flight and hence range to be unambiguously determined.

Data was recorded at five photocount (recorded events originating from actual return photons and not background or dark counts) levels of the SPAD: 1000 counts per second (c/s), 5000c/s, 10 000c/s, 50 000c/s and 100 000c/s for a fixed background count rate of 100 000c/s. For each count rate a total of 100 000 time-stamps were recorded. The received patterns were determined and the required number of pattern steps to re-align the transmitted and received patterns was found in each case. A graph of the number of correlating bits from a comparison of all 100 000 recorded time-stamps against number of indices subtracted from the received pattern is shown in Fig. 2. The measurement time to record the 100 000 time-stamps depended on the combined count rate of the photocounts, background counts and the dark counts of the SPAD. The measurement times were 1011.9ms (Photocount rate (PCR) ~1000c/s); 969.2ms (PCR ~ 5000c/s); 932.1ms (PCR ~ 10 000c/s); 693.1ms (PCR ~ 50 000c/s) and 526.9ms (PCR ~ 100 000c/s). This measurement time information and the length of each transmitted pattern, 96μs, revealed the number of repeated pattern transmissions for each measurement.

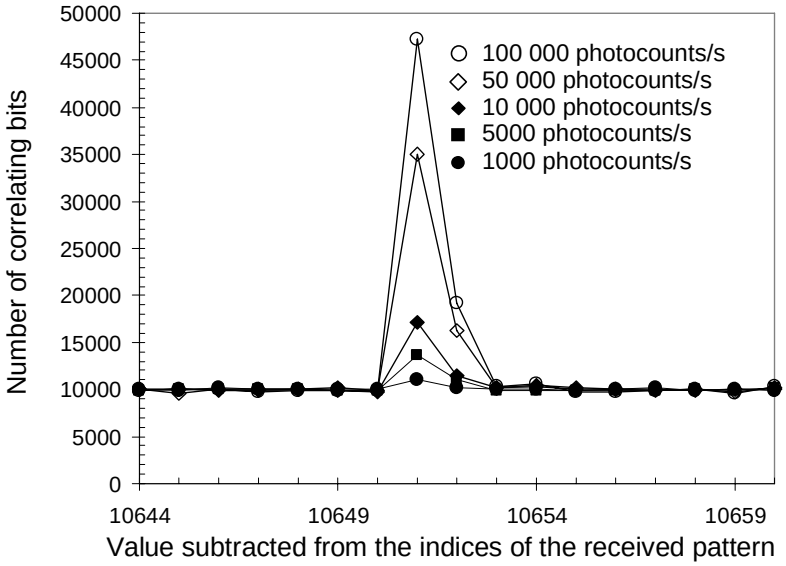


Fig. 2. A graph of the number of correlating bits between the transmitted and received patterns against number of pattern steps for 5 different photocount levels. At each step position, all 100 000 bits in the received pattern were compared to the corresponding bits in the transmitted pattern.

#94106 - $15.00 USD Received 20 Mar 2008; revised 27 Jun 2008; accepted 23 Jul 2008; published 21 Aug 2008

Figure 2 shows a strong level of correlation when the received pattern was offset by 10651 clock periods but there is also a smaller correlation at the neighboring clock period, 10652. Another important feature of the figure is that the baseline correlation level of ~10 000 bits from the 100 000 bits compared at each offset. This was a consequence of the random number threshold which determined the probability of a laser pulse per clock period being 0.1. For each bit in the received pattern, regardless if the transmitted and received patterns were correctly aligned or not, there was always a probability of 0.1 that the transmission pattern also contained a one value. This probability level was originally selected in order to observe a clear correlation peak in the presence of background, despite the trade-off with a lower count rate.

The increased level of correlations at 10652 was an artifact of the time response of the overall photon-counting system. The time-stamped detected photon events had a time distribution around a central peak due to the overall jitter of the photon-counting system. In these experiments, the primary causes of jitter are the SPAD jitter (~400ps FWHM), the temporal width of the laser pulse jitter (~100ps FWHM), and the timing response of the TSB (the TSB time-stamps events to ~75ps jitter). This timing distribution of the detected photon events was measured to have a FWHM of 440ps**,** as shown in Fig. 3. Note that in this specific measurement of the system jitter, the experiment was configured using a periodic pulse train, and Fig. 3 shows the time-tagged photon events being displayed in a histogram format. The range-finding measurements and analysis presented in this paper were performed using the previously described set-up using pseudorandom pulse trains.

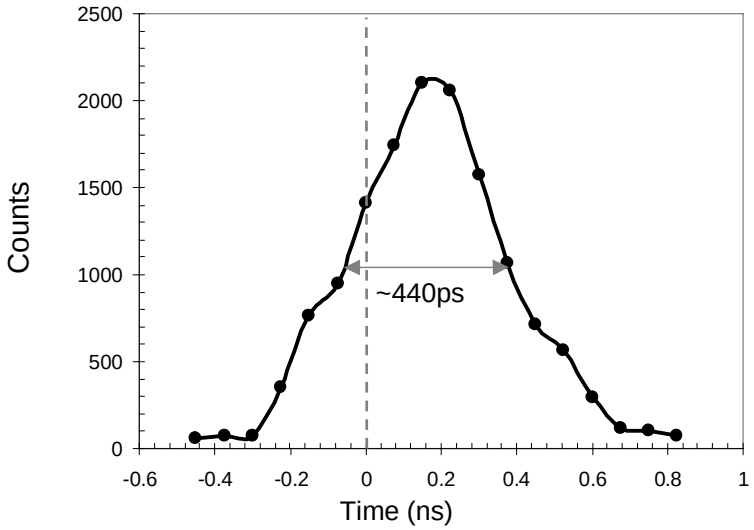


Fig. 3. The timing response histogram of the time-stamped detected photon events, illustrating a system jitter of 440ps (FWHM)

The time-stamp values of the detected photon events from the transmitted laser pulse were distributed over this time distribution with essentially all the values being distributed within a 1ns time interval. This set the upper limit to the clock repetition rate of this particular system to 1GHz. A system with lower jitter would have permitted a higher clock frequency to be used and an improved temporal resolution achieved by the coarse pattern recognition approach without further processing of data.

Consider a photon detected in the $n^{th}$ period after the TSB was armed. The position of this $n^{th}$ period is represented by the dashed line in Fig. 3. It was explained earlier that each time-stamp is assigned to the nearest 1ns-clock reference; a time-stamp with a value within ± half a

#94106 - $15.00 USD Received 20 Mar 2008; revised 27 Jun 2008; accepted 23 Jul 2008; published 21 Aug 2008

clock period of the $n^{th}$ clock period will be assigned to the $n^{th}$ index. The centroid of the timing distribution of the time-stamped detected photon events need not be aligned to a 1ns-clock reference and therefore some time-stamps can be assigned to the $(n+1)^{th}$ index (as is the case in Fig. 3) or the $(n-1)^{th}$ index depending on the position of the centroid with respect to the $n^{th}$ index. The position of the centroid of the timing response in Fig. 3 relative to the clock period corresponded to the case shown in Fig. 2. Some of the time-stamps that belong in the $n^{th}$ index had values just greater than + half a clock period of the $n^{th}$ clock period and, therefore, were assigned to the next index value instead of the correct value. During the cross-correlation process, these incorrectly assigned indices required that the received pattern be offset by an additional index for correlation to occur, as in the case in Fig. 2. For systems where the clock period is much greater than the response of the system, then it is unlikely that more than one offset of the received pattern relative to the transmitted pattern will show correlation because this will only occur if the timing response of the arriving photons is coincident with the mid-way position between two 1ns-clock references.

Unlike traditional TAC-based measurements where arrival times are binned and a timing histogram is formed, similar to that shown in Fig. 3, the results in this paper did not rely on the histogramming of received time-stamps. Figure 3 provides a useful guide to those unfamiliar with the instrumental response of a TCSPC system to illustrate the uncertainty in the measured arrival times of single photon returns in this experiment. Typically in TCSPC applications, counts are recorded and histogrammed into bins of width far narrower than the instrumental time of the SPAD detector, for example as shown in [2]. The results presented in this paper are recorded using a TSB with a timing jitter of ~75ps which contributed to the overall system jitter of 440ps FHWM. Other contributions to this overall instrumental response include those from the detector, the laser and other components in the system as described above.

The simple technique described above provides time-of-flight to a time resolution equivalent to that of the clock period, in this case 1ns. After this stage the resolution was further improved by using a windowing approach to improve the time resolution to that of the instrumental response function (~440ps FWHM in this case). To achieve this, an integer number of small increments (50ps in this case) were successively subtracted from each time-stamp value in post-processing. At each increment, the modified time-stamp value was retained if and only if it was within a selected measurement timing window centered on a 1ns-clock reference, otherwise the time-stamp was ignored. The timing window was selected to be of approximately equivalent width, or slightly narrower, than the FWHM of the system instrumental response. For the initial analysis shown below we chose a measurement timing window of ±200ps. If the bit was retained it was assigned an index value and a received pattern is formed. At each increment, each bit in the received pattern was compared to the corresponding bit in the transmitted pattern and the number of correlations determined. When the time subtracted from the raw timestamps was equivalent to the time-of-flight an increased level of correlation was observed.

Since the approximate time-of-flight was previously determined using the coarse technique to be within the range 10650ns to 10653ns, then we only need use the higher resolution technique in that particular range. Figure 4 is a graph of number of correlating bits against time-of-flight from analysis of the 100 000 raw time-stamps used for Fig. 2 from which 10 000 bits were randomly chosen after windowing to form the received pattern. The total measurement time for the 100 000 raw time-stamps was, therefore, the same as those for Fig. 2.

#94106 - $15.00 USD Received 20 Mar 2008; revised 27 Jun 2008; accepted 23 Jul 2008; published 21 Aug 2008

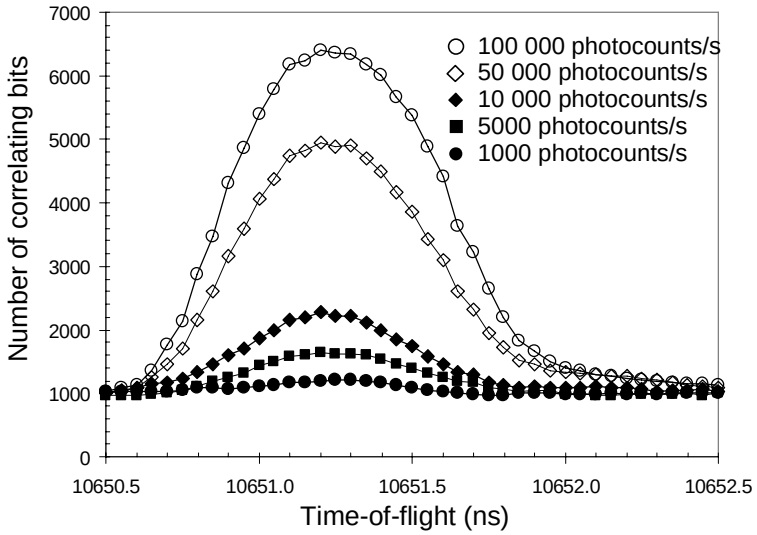


Fig. 4. A graph of the number of correlating bits (in 10 000 random comparisons of post-windowed bits) between transmitted and received patterns against time-of-flight for five photocount levels at a background count rate of 100 000 c/s. As described in the text, the raw time-stamps were modified by the subtraction of a time value between 10650ns and 10653ns in steps of 50ps. A bit value was retained if it coincided with a window of width ±200ps centered on the 1ns-clock reference. For each step, the retained bits form the received pattern and the number of correlating bits between the transmitted and received patterns was determined. The subtracted time value that yields the highest correlation corresponds to the time-of-flight..

The peak in the 100 000 photocounts/s curve can be seen to be (10651.20 ± 0.05) ns, corresponding to a range of (2208.27± 0.01)m (using 1.447 as the refractive index value of the fiber).

An important feature of the results shown in Fig. 4 is the baseline correlation level. This baseline correlation level is caused by the random number threshold of 0.1 and not the level of the background count rate. A time-of-flight measurement system is required to be tolerant to high background count rates since, typically, ranging systems are required to work in daylight conditions and the presence of the high solar background level usually dominates the background level, as shown in [2]. The effect of increased background count rate on the system is a reduction the number of correct correlations for a given window size. To demonstrate this, the photocount rate was set to 10 000 c/s and the time-of-flight was investigated with background count rates of 25 000 c/s, 50 000 c/s, 100 000 c/s and 500 000 c/s. This was done by using the coarse approach, followed by the higher resolution approach described above. For each background rate, 100 000 raw time-stamps were recorded, these time-stamps were windowed using a ±200ps window and 10 000 post-windowed timestamps were used to find the time-of-flight. The measurement times were 2874.4ms (background rate ~25 000c/s); 1695.3ms (background rate ~50 000c/s); 932.1ms (background rate ~100 000c/s) and 218.3ms (background rate ~500 000c/s). The results are shown in Fig. 5.

#94106 - $15.00 USD Received 20 Mar 2008; revised 27 Jun 2008; accepted 23 Jul 2008; published 21 Aug 2008

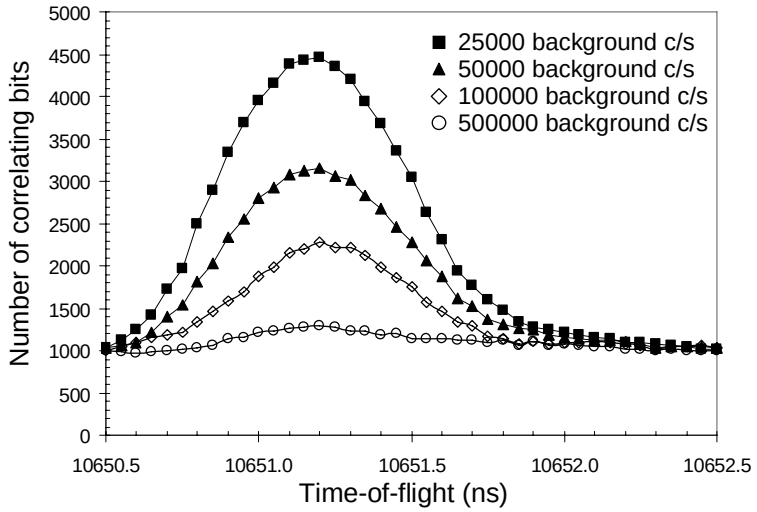


Fig. 5. A graph of the number of correlating bits (in 10 000 random comparisons of post windowed bits) between transmitted and received patterns. In this case, four different background levels are shown of 25 000 c/s, 50 000 c/s, 100 000 c/s and 500 000 c/s using the same analysis technique used in Fig. 4.

Background counts occur randomly and are distributed uniformly across each 1ns clock period - unlike the return photons which have a specific timing distribution. A narrow measurement window applied to the raw time-stamp values can retain a disproportionately higher number of photocounts compared to the number of background/dark counts that are coincident with the timing window. Figure 6 is a graph of the number of correlations (in 10 000 random comparisons of post-windowed bits) between transmitted and received patterns against time-of-flight analyzed at four window widths. The photocount rate was 10 000 c/s and the background count rate was 100 000 c/s.

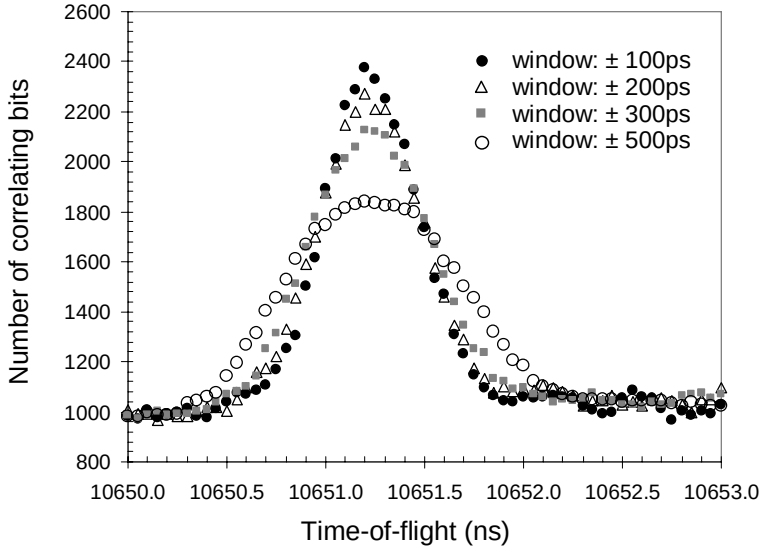


Fig. 6. A graph of the number of correlating bits (in 10 000 random comparisons) between transmitted and received patterns against time-of-flight analyzed at four different window widths of ± 100ps, ± 200ps, ± 300ps and ± 500ps. The photocount rate was 10 000c/s, the background count rate was 100 000 c/s and 100 000 time-stamps were recorded in all cases.

#94106 - $15.00 USD Received 20 Mar 2008; revised 27 Jun 2008; accepted 23 Jul 2008; published 21 Aug 2008

For each window width, a total of 100 000 raw time-stamps were recorded and, therefore, the overall measurement time was the same for each width. However, the window width determined the number of bits that were retained after windowing and, therefore, the post-windowed 'bit rate' (the number of post-windowed bits retained from the 100 000 raw time-stamps acquired in the measurement time) was dependent on the window width. For the results shown in Fig. 6, only 10 000 post-windowed bits were randomly selected for each width, which for larger window widths (where significantly more than 10 000 bits were retained after windowing) lead to many 'useful' post-windowed bits being discarded. It may be desirable for future work to optimize the measurement time for a given windowing condition (which is dependent on the photocount and background count rates) so that data collection only occurs until enough raw time-stamps are acquired to yield the desired number of post-windowed bits.

The window width of ±200ps was selected to reduce the effect of the background rate of 100 000 c/s. This window width, equivalent to 40% of a clock period combined with the large number of raw time-stamps recorded, 100 000, enabled the extraction of 10 000 post windowed bits for comparison regardless of the time increment applied to the raw time-stamps. In conditions where the background count is high and the photocount rate is low then narrow window widths will increase the likelihood of extracting time-of-flight data. For the results shown in Fig. 5 where results are shown for a background count rate of 500 000 c/s it was found that a window of width greater than ±200ps did not yield time-of flight data for a photocount of 10 000 c/s.

The technique was then tested over a free-space range of approximately 330m. The optical system, shown in Fig. 7, was a simplified version of the optical system previously reported by Buller et al [2].

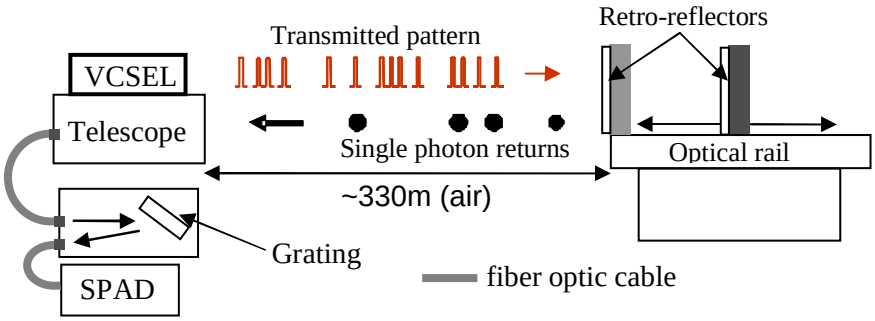


Fig. 7. The optical arrangement of the free-space ranging system. The VCSEL was mounted on the rim of the telescope and was triggered by the same randomly produced pattern as used in the fiber experiment. The output of the VSCEL was collimated and aligned onto the retro-reflectors.

This optical system was based on a 210mm diameter Schmidt-Cassegrain telescope and used a single VCSEL source mounted on the outer rim of the telescope. The output from the VCSEL was collimated and directed at two retro-reflecting corner cubes which were mounted on an optical rail and placed on a concrete pillar ~330m from the telescope. One cube was held in a fixed position at the front of the rail whilst the other cube's position was variable over an 80cm length of the rail. The returns were collected by the telescope optics and coupled into a 100µm diameter optical fiber and then filtered using a diffraction grating which passed only the spectral region (850.0 ± 5.5)nm to a silicon SPAD detector.

Two experiments were performed using this experimental arrangement. In the first experiment, only the moveable retro-reflecting cube was used and the fixed cube was covered. The moveable cube was positioned at 11 different positions along the rail and the range measured at each position. In the second experiment, both cubes were exposed and the time-of-flight was measured simultaneously for the fixed front cube and the moveable cube

#94106 - $15.00 USD Received 20 Mar 2008; revised 27 Jun 2008; accepted 23 Jul 2008; published 21 Aug 2008

positioned at various distances along the rail to determine both the range and surface-to-surface resolution. This second experiment was analogous to an object with two surfaces.

For both experiments, the pattern recognition technique was used first to identify the coarse time-of-flight and then the raw time-stamps were used to investigate the time-of-flight to a higher temporal resolution using the subtraction technique used earlier. The average output power of the VCSEL, which was pulsed on average $1x10^8$ times per second, was 50nW. The data was taken at night and the weather conditions were high winds, no rain and the temperature was just above freezing. These weather conditions caused a degree of "scintillation", i.e. changes in the average photon count signal – where the turbulence caused small changes in the optical paths on the millisecond timescale. The optical system was of a bistatic design, originally designed for the collection of light scattered from a Lambertian reflector: the use of retro-reflectors significantly enhanced the effects of scintillation in this demonstration. The measurements were taken in dark conditions to avoid changes in the solar background level, however previous measurements [2,3] indicate that daylight measurements can be routinely achieved with appropriate spatial and spectral filtering.

Figure 8 shows a graph of the number of correlating bits obtained against time-of-flight for the moveable corner cube at various positions along the optical rail with the fixed cube covered. During the measurements, the photocount rate was seen to fluctuate between ~10 000 c/s and ~50 000c/s. The average count rate (photocount and background rate) was recorded using a Stanford SR400 photon counter during the measurement process and was found to be 10 800 c/s (0cm); 14 500 c/s (5cm); 17 500 c/s (10cm); 32 000c/s (25cm); 20 000c/s (40cm) and 38000c/s (60cm). The raw time-stamps were modified by the successive subtraction of 50ps increments between 2196ns and 2204ns. For each stepped value, the modified time-stamps were windowed by the application of a ±500ps measurement window at the 1ns-clock reference positions. The low background conditions allowed the selection of this maximum window width. Each post-windowed bit was assigned an index value and a received pattern formed. At each step, the transmitted and received patterns were compared and the number of correlations measured for *all* the 100 000 post-windowed stamps (all stamps are retained in this case because the window was ±500ps). The step position which yields the maximum number of correlations was the measured time-of-flight. The use of all the time-stamps averages out the effects of scintillation and the corresponding fluctuation in the count rate of the SPAD.

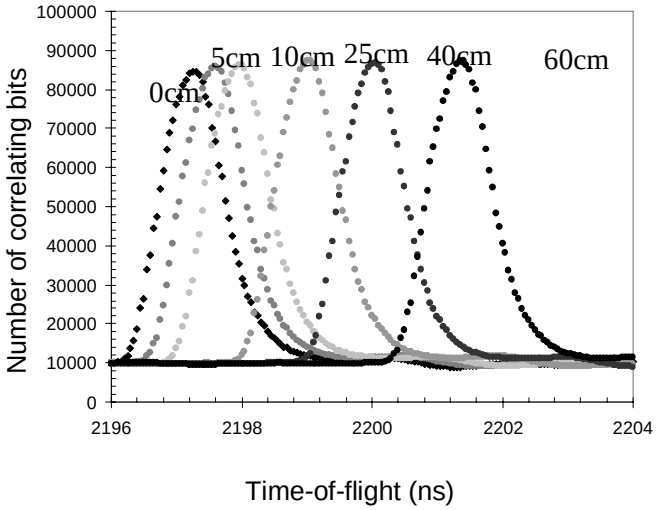


Fig. 8. A graph of number of correlations against time-of-flight for 6 example positions of the moveable corner cube along the optical rail (for clarity only 6 from the 11 recorded returns are shown). As in Fig. 4, the raw time-stamps were modified by the successive subtraction of 50ps increments between 2196ns and 2204ns. The timing window used was ±500ps. The front corner cube was obscured for these experiments.

#94106 - $15.00 USD Received 20 Mar 2008; revised 27 Jun 2008; accepted 23 Jul 2008; published 21 Aug 2008

The peak of each of the curves was found and the corresponding range calculated. Figure 9 shows the graph of measured range against relative position of the moveable corner cube to the fixed cube along the optical rail. The standard deviation of the measured values from the reference line of unity gradient was 3.5mm.

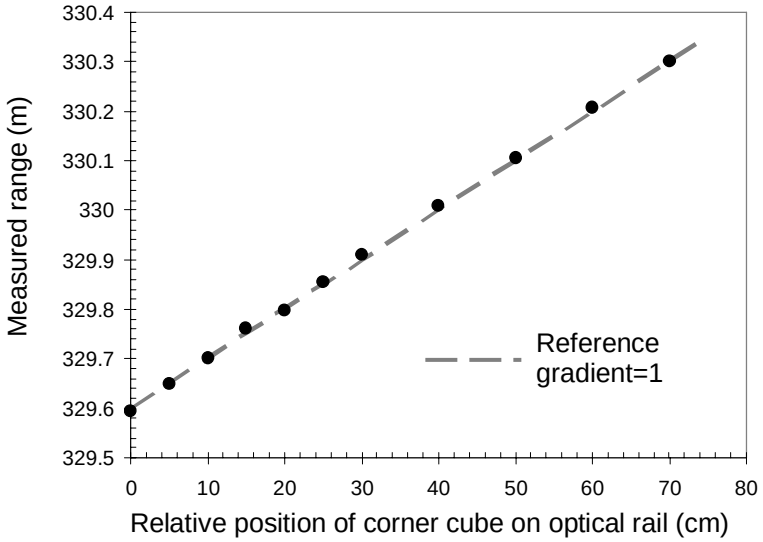


Fig. 9. A graph of the measured range using the technique shown in Fig. 8 against the relative position of the moveable corner cube. .

For the second experiment, the fixed corner cube was uncovered and the position of the moveable cube varied as before, in order to determine the surface-to-surface depth resolution of the system. The return from each cube had an associated timing response of the SPAD and the TSB. As the separation of the two corner cubes was reduced, the timing response histograms of the two returns began to overlap and it became progressively more difficult to resolve the separations of the two returns, as shown in Fig. 10.

During this investigation it was clearly observed that not only did the total number of returns coupled into the telescope fluctuate because of scintillation but also the level of returns from each individual corner cube varied over the measurement time. This made the effects of scintillation more pronounced in this experiment since photon events from the returns from both targets were required simultaneously. If only a small number of time-stamps were taken and then processed, the number of correlations from the returns from each cube was seen to vary significantly between acquisitions.

The simplest approach to addressing this problem was to acquire data over longer measurement times so as to average out the scintillation effects. Therefore, 750 000 raw time-stamps were recorded instead of the 100 000 for the single cube case. For each separation, a coarse measurement was taken to identify the approximate time-of-flight, and as before, the raw time-stamps were then modified by successively subtracting 50ps increments between 2196ns and 2204ns..The background count rate when the data was collected was 600c/s, with this low background level a ±500ps window was centered on the 1ns-clock reference. With this window width all the time-stamps were retained in the windowing and were, therefore, used in the measurement of correlation between the transmitted and received patterns for eight separation distances of the corner cubes. The average count rate (photocount and background count rate) was measured to be 28 500c/s (10cm), 34 000c/s (30cm) and 40 500c/s (70cm). Figure 10 shows the results for the corner cubes separated by three of the eight separation distances: 10cm, 30cm and 70cm. Also shown in the figure is the result for the 10cm separation using a smaller ±100ps timing window.

#94106 - $15.00 USD Received 20 Mar 2008; revised 27 Jun 2008; accepted 23 Jul 2008; published 21 Aug 2008

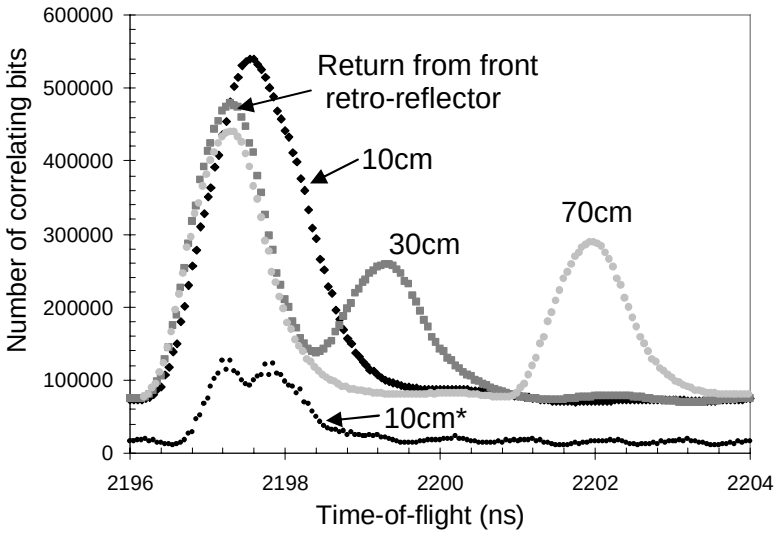


Fig. 10. Graphs of the number of correlating bits between transmitted and received patterns against time-of-flight. The raw time-stamps were modified by subtracting time values between 2196ns and 2204ns in steps of 50ps. The window width was ±500ps centered on the 1ns-clock reference so that all the bits were retained. Also shown is the result for the 10cm separation (labeled 10cm*) obtained using a ±100ps timing window, all the post windowed bits were used to determine the time-of-flight. For clarity, not all separation distances are shown.

Figure 10 shows that for a window width of ±500ps that the returns from the two corner cubes when separated by 10cm could not be resolved, this was also found to be the case for the separation of 15cm. To determine the separation at 10cm and 15cm the window width was required to be reduced to ±100ps (10cm) and ±200ps (15cm). The time-of-flight values measured in Fig. 10 were used to calculate the separation of the corner cubes. A graph of the measured corner cube separation against actual corner cube separation is shown in Fig. 11.

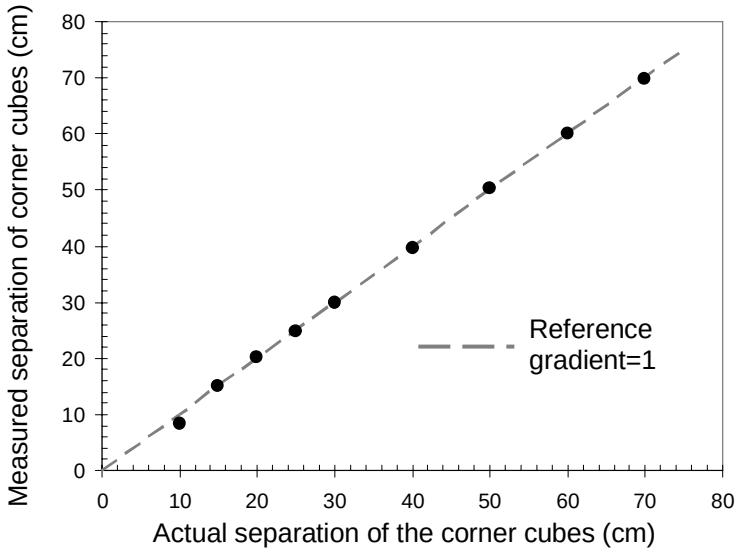


Fig. 11. Graph of measured separation of the two corner cubes against actual separation. A best fitting straight line with unity gradient is shown. The separation was measured using a ±500ps measurement window for all points except for 10cm and 15cm which were determined using a ±100ps and a ±200ps window respectively.

#94106 - $15.00 USD Received 20 Mar 2008; revised 27 Jun 2008; accepted 23 Jul 2008; published 21 Aug 2008

For the situation where the separation between the two cubes was 5cm it was not possible to resolve the separation of the two cubes from the time-of-flight data. The standard deviation of the data points from the reference line with unity gradient was measured to be 5.5mm.

In previous TCSPC measurements [11] using periodic pulsed sources, the uncertainty in depth follows the expected dependency with the number of target return counts. The uncertainty in these time-of-flight measurements obtained with the measurement technique described above depends on the instrumental response of the system, the step size applied to the raw time-stamp value, the size of the measurement window and the correlation between the transmitted and received patterns (which depends on the total recorded bits). It is clear that a system with reduced system jitter would allow more accurate measurement of the time-of-flight. The precise conditions for measurement of the time-of-flight have been shown to depend on the photocount rates, background count rates and the distribution of the returns and the optimum conditions for these measurements and their associated uncertainties requires further detailed investigation.

## 3. Conclusions and further work

We have demonstrated that a pattern recognition technique, which is analogous to a similar scheme used in radar can be successfully adapted to unambiguously determine the time-of-flight in a high clock rate photon-counting time-of-flight system. We have demonstrated this approach in laboratory-based optical fiber experiments over ~2.2 kilometers and in free-space time-of-flight experiments over a range of ~330 meters.

An unambiguous initial estimate of the range was obtained with a cross-correlation of the transmitted and received patterns. It was shown that, typically, there was evidence of correlation in an adjacent clock cycle because the centre of the timing distribution of the detected photons from the returns was not coincident with a clock period. The timing response, however, of the detector used in this work and the jitter of the TSB limited the clock rate of the system to 1GHz. Alternative silicon SPADs are capable of ~35ps FWHM [12], compared to the ~400ps FWHM of the detectors used in this work, which proved to be the largest contribution to jitter in these measurements. A higher clock rate would enable improved range resolution using just the coarse pattern recognition technique.

A powerful advantage of this coarse pattern recognition technique is the capability to range multiple objects along the transmission path. There will be an increased level of correlation between the transmitted and received patterns at different offset positions from each object along the range. The return from any particular object can be independently investigated using an improved resolution technique once its offset is revealed by the coarse pattern sweep. A simple post-processing technique to extract improved temporal resolution time-of-flight data was described in this paper.

The results shown in Fig. 4 and Fig. 5 show that the pattern recognition technique can yield time-of-flight information for situations where there are low photon returns and/or high background count rates. The random number threshold determined the probability that the VCSEL was pulsed in each clock period and therefore the transmitted pattern was ‘tagged’ [10] in terms of amplitude, i.e. a 1 bit represented the VCSEL being pulsed in a clock period, a 0 bit represented the VCSEL not being pulsed in a clock period. The threshold of 0.1 was chosen for these experiments because it demonstrated a high number of pulses in the transmission line at any instant and this is the primary aim of this work to demonstrate unambiguous ranging. This 0.1 value, however, caused a background correlation of 10% of the number of compared bits because when the patterns were misaligned, for every received bit in the received pattern there was a probability of 0.1 that there was a 1 value in the transmitted pattern. This reduces the sensitivity of the system. Ideally we would like to increase the number of pulses in flight to increase the data acquisition rate and also maintain a sufficiently low background correlation level to be able to extract low levels of returns at high background count rates. One simple solution to increase the number of laser pulses in the transmission line would be to improve the timing resolution of the SPAD and timing

#94106 - $15.00 USD Received 20 Mar 2008; revised 27 Jun 2008; accepted 23 Jul 2008; published 21 Aug 2008

electronics so that the clock rate of the system could be increased above 1GHz. This increases the number of pulses in flight and does not reduce the intrinsic background correlation level which is determined by the random number threshold: unless with the higher clock rate system, the random number threshold is reduced to maintain the number of pulses in flight at the level of the 1GHz system and therefore reduce the background correlation level.

It appears that there is a trade-off between the number in pulses in flight and the system sensitivity for a fixed clock rate. The random number threshold determines the bin filling of the transmitted pattern and therefore the transmitted pattern is "tagged" [10] in terms of amplitude. We can however apply a secondary tag to each transmitted pulse by applying an additional level of encoding. At the time of detection this additional coded information is read. Therefore, when the level of correlation between the received and transmitted pattern is investigated, it is not just a matter of whether the laser was pulsed in the corresponding index in the transmitted pattern but also, if the laser was pulsed, was the transmitted pulse "tagged" in the same way as the received photon. An example of additional encoding would be to randomly encode the transmitted photons in terms of wavelength where two lasers of differing wavelengths would be used. In a given clock cycle the random number threshold determines if a laser pulses and an additional random process determines which one of the two lasers is pulsed in that clock period. The returning single photons are 'decoded' by separating the wavelengths by a diffraction grating or dichroic mirror and then detected by a separate SPAD for each wavelength. The returns at each wavelength are time-stamped and a received pattern is formed where each detection event is assigned an index value and is tagged with the corresponding wavelength. During the comparison between each event in the received pattern and the corresponding clock period in the transmitted pattern a correlation is only registered if firstly, the laser was pulsed in that period and secondly, if the wavelength tags match. For a random number threshold, i.e. the probability that *one* of the two lasers are pulsed in a single clock period, of 0.1 and the additional random encoding introduced by using two lasers, one for each wavelength, would reduce the background correlation level to 0.05. An alternative interpretation of this example is that to maintain a background correlation level of 0.1, the random number threshold can be increased to 0.2.

This paper has investigated approaches for the avoidance of range ambiguity in photon-counting time-of-flight – approaches that may prove essential if the full potential of high clock rate TCSPC is to be utilized in time-of-flight ranging, depth imaging and target identification systems.

**Acknowledgments**

The authors would like to thank Ron Lau of GuideTech for many helpful discussions. We also acknowledge useful discussions with Prof Robert Lamb of SELEX, Basildon. The authors acknowledge the financial support of the UK Electro-Magnetic Remote Sensing (EMRS) Defense Technology Centre established by the UK Ministry of Defence and run by a consortium of SELEX Galileo, Thales UK, Roke Manor Research and Filtronic.

#94106 - $15.00 USD Received 20 Mar 2008; revised 27 Jun 2008; accepted 23 Jul 2008; published 21 Aug 2008